Eur J Nucl Med Mol Imaging (2014) 41:2212–2221
DOI 10.1007/s00259-014-2867-7

ORIGINAL ARTICLE

Use of diffusion-weighted imaging (DWI) in PET/MRI for head and neck cancer evaluation

Marcelo A. Queiroz · Martin Hüllner · Felix Kuhn · Gerhardt Huber · Christian Meerwein · Spyros Kollias · Gustav von Schulthess · Patrick Veit-Haibach

Received: 5 March 2014 / Accepted: 16 July 2014 / Published online: 5 August 2014

Abstract
Objective The purpose of this study was to analyze whether diffusion-weighted imaging (DWI) adds significant information to positron emission tomography/magnetic resonance imaging (PET/MRI) on lesion detection and characterization in head and neck cancers.
Methods Seventy patients with different head and neck cancers were enrolled in this prospective study. All patients underwent sequential contrast-enhanced (ce) PET/computed tomography (CT) and cePET/MRI using a tri-modality PET/CT-MR setup either for staging or re-staging. First, the DWI alone was evaluated, followed by the PET/MRI with conventional sequences, and in a third step, the PET/MRI with DWI was evaluated. McNemar's test was used to evaluate differences in the accuracy of PET/MRI with and without DWI compared to the standard of reference.
Results One hundred eighty-eight (188) lesions were found, and of those, 118 (62.8 %) were malignant and 70 (37.2 %) were benign. PET/MRI without DWI had a higher accuracy in detecting malignant lesions than DWI alone (86.8 % vs. 60.6 %, $p<0.001$). PET/MRI combined with DWI detected 120 concurrent lesions (89 malignant and 31 benign), PET/MRI alone identified 48 additional lesions (20 malignant and 28 benign), and DWI alone detected 20 different lesions (nine malignant and 11 benign). However, lesions detected on DWI did not change overall staging. SUV maximum and mean were significantly higher in malignant lesions than in benign lesions. DWI parameters between malignant and benign lesions were not statistically different.
Conclusion The use of DWI as part of PET/MRI to evaluate head and neck cancers does not provide remarkable information. Thus, the use of DWI might not be needed in clinical PET/MRI protocols for the staging or restaging of head and neck cancers.

Keywords PET/MRI · DWI · Head and neck cancer · SUV · ADC · b-value

M. A. Queiroz (✉) · M. Hüllner · F. Kuhn · G. von Schulthess · P. Veit-Haibach
Department of Medical Radiology, Nuclear Medicine, University Hospital Zurich, Zurich, Switzerland
e-mail: marcelo.araujoqueiroz@gmail.com

F. Kuhn · P. Veit-Haibach
Department of Medical Radiology, Diagnostic and Interventional Radiology, University Hospital Zurich, Zurich, Switzerland

M. Hüllner · S. Kollias
Department of Medical Radiology, Neuroradiology, University Hospital Zurich, Zurich, Switzerland

G. Huber · C. Meerwein
Department of Otorhinolaryngology, University Hospital Zurich, Zurich, Switzerland

Introduction

Head and neck cancers (HNC) are among the most prevalent cancers, accounting for more than 550,000 cases annually worldwide [1]. The primary risk factors associated with HNC include tobacco use, alcohol consumption, human papillomavirus (HPV) infection (for oropharyngeal cancer), and Epstein-Barr virus (EBV) infection (for nasopharyngeal cancer) [2]. Standard treatments for head and neck cancers include radiation therapy and surgery, and for certain types of head and neck cancer, chemotherapy. Survival is partly poor and has partly improved over the past three decades [3], possibly related to a better tumor staging system and a strict follow-up protocol, including the imaging approach.

^{18}F-fluorodeoxy-D-glucose (FDG) positron emission tomography/magnetic resonance imaging (PET/MRI) appears to be an excellent tool for imaging evaluation of head and neck cancers due to the high soft-tissue contrast provided by the MR component and the possibly better characterization of HNC. The definition of MR protocols for PET/MRI is challenging due to the vast amount of differently weighted sequences, but acquisition time should ideally be no longer than a standard PET/CT with contrast media. Furthermore, because of the availability of the PET component, the information provided by the MR component should be complementary or confirmatory to the PET information, but not redundant.

Diffusion-weighted imaging (DWI) was initially established as a functional MR technique that helps in detecting acute stroke, and has been researched for a wide variety of extracranial applications as well [4, 5]. It analyses the structure of a biologic tissue at a microscopic level based on the motion of water molecules. The differences in water mobility are quantified by an apparent diffusion coefficient (ADC). The ADC reflects the signal loss on DWI that occurs with increasing b-values and is inversely correlated with tissue cellularity [6–8].

FDG is a glucose analogue that accumulates in tumor cells after its transformation to FDG-6-phosphate by hexokinase, which cannot be oxidized further through glycolysis [9]. The semi-quantitative assessment of the glucose metabolism in these cells is expressed by the standardized uptake value (SUV). The SUV is defined as the FDG uptake in a tumor over a certain time interval, considering tracer decay, the administered dose of the PET tracer, and the patient's body weight [10].

In HNC, DWI has been widely used for tissue characterization for primary tumors and lymph node (LN) metastases, prediction and monitoring of treatment response, and differentiation of recurrent tumors from post-therapeutic changes [11]. However, even if DWI and FDG do show different molecular phenomena, in the context of PET/MRI with the FDG-PET component available, the additional DWI component might actually represent redundant information to FDG-PET. Furthermore, one study has shown that DWI does not improve lesion detection in a PET/MRI protocol for whole-body cancer staging in a mixed oncologic population [12].

Thus, the aim of this study was to analyze whether the addition of a DWI sequence to PET/MRI adds significant additional information concerning lesion detection and characterization in patients with head and neck cancer.

Materials and methods

Patient population

A total of 157 adult patients who underwent PET/CT-MR between February 2012 and March 2013, either for staging or re-staging of various head and neck cancers, were enrolled in this prospective study. The inclusion criterion was the presence of at least one suspicious lesion on full-diagnostic PET/MRI, regardless of the type of treatment for recurrent lesions. The exclusion criteria of the present study included: unwillingness to undergo an additional MR exam, claustrophobia, MR-incompatible medical devices (e.g., cardiac pacemakers, neurostimulators, cochlear implants, and insulin pumps), or possible metallic fragments in the body. The institutional ethics committee approved this study and signed informed consent was obtained from all subjects prior to the examination.

PET/CT and MR imaging

Sequential PET/CT, ceCT, and ceMR were performed on a trimodality PET/CT-MRI setup (full ring, time-of-flight Discovery PET/CT 690, 3T Discovery MR 750 w, both GE Healthcare, Waukesha, WI, USA). The dedicated MR- and CT-compatible shuttle transfer mechanism connecting the MR system and the PET/CT system allowed for PET/CT scanning that was free of radiofrequency (RF) coil-induced artifacts, and also made it possible to ascertain the placement of dedicated RF coils for MR imaging without repositioning of the patient [13, 14].

In accordance with the European Association of Nuclear Medicine (EANM) procedure guidelines for PET imaging, patients fasted for at least 4 h prior to injection of a standard dose of 4.5 MBq per kg body weight [15]. After an uptake time of 30 min, the patients were positioned on the shuttle table in the MR suite and the MR acquisition covering the region between the orbital roof and the cranial end of the sternum was initiated. The images were acquired using a dedicated RF coil (32-Channel HD Head-Neck-Spine, GE Healthcare). The applied MR pulse sequences (PS) included an axial, T1-weighted (T1w), three-dimensional (3D), spoiled-gradient echo pulse sequence (LAVA), an axial, two-point, Dixon-based, T2-weighted (T2w) gradient echo sequence (IDEAL), an axial, two-point, Dixon-based, ceT1w-gradient echo sequence (IDEAL), coronal and sagittal, two-point, Dixon-based, ceT1w-gradient echo sequences (LAVA flex), and an axial DWI. All images were acquired with a slice thickness of 4 mm within a total duration of the MR of 20–25 min (additional scanning parameters are listed in Table 1). The intravenously (IV) injected amount of contrast medium (Omniscan, GE Healthcare) was 0.2 mL/kg body weight at a flow rate of 1.5 ml/s. After completion of the MR scan, the coils were removed and the patient was transferred to the PET/CT scanner, still being positioned on the shuttle board. This ensures an identical position of the patient during the acquisition of both the PET/CT and the MR exam.

Non-enhanced low-dose CT and PET emission data were acquired from the mid-thigh to the vertex of the skull.

Table 1 MR acquisition parameters

Parameter	T1w LAVA	T2w IDEAL	ceT1w LAVA flex	DWI EPI-STIR
Repetition time/echo time (ms)	8.1/2.1	5188/80	6.2/1.7	5500/66.1
Echo train length	NA	23	NA	NA
Flip angle (°)	15	90	15	90
Inversion time (ms)	NA	NA	NA	250
Parallel imaging acceleration factor	2	2	2	2
Receiver bandwidth (kHz)	83.33	83.33	166.67	250
Field of view (cm)	24	24	24	24
Matrix	320×256	320×256	220×220	320×256
b-value (s/mm)	NA	NA	NA	0 and 800
NEX	NA	NA	NA	1
Number of directions	NA	NA	NA	3
Acquisition time	00:57	03:38	03:50	01:39

T1w LAVA T1-weighted, spoiled-gradient echo pulse sequence; *T2w IDEAL* Two-point, Dixon-based, 3D T2-weighted gradient echo sequence; *ceT1w IDEAL* Two-point, Dixon-based, 3D contrast-enhanced, T1-weighted gradient echo sequence; *ceT1w LAVA flex* Two-point, Dixon-based, 3D contrast-enhanced, T1-weighted gradient echo sequence; *DWI* Diffusion-weighted imaging sequence; *EPI-STIR* Echo planar imaging–short-time inversion recovery; *NEX* Number of excitations; *NA* Not applicable

PET data was acquired in 3D time of flight (TOF) mode with a scan duration of 2 min per bed position, an overlap of bed positions of 23 %, and an axial field of view (FOV) of 153 mm. The emission data was corrected for attenuation using the low-dose CT (CTAC), and was then iteratively reconstructed (matrix size 256×256 pixels, Fourier rebinning (VIP mode), VUE Point FX (3D) with three iterations, 18 subsets).

Image processing

The acquired PET, CT, and ceMR images were transmitted to a dedicated review workstation (Advantage Workstation, Version 4.5, GE Healthcare), which enables the review of the PET, CT, and ceMR images side by side or in fused/overlay mode (PET/CT; cePET/MRI). Due to the calibrated trimodality system, no software-based image registration was necessary. A previously conducted study validated the image registration accuracy with less than 4 mm of lateral misalignment between CT, PET, and MR data sets, similar to the intrinsic error assessed with phantom measurements [16].

Image analysis

All images were analysed in consensus by a board-certified nuclear medicine physician/radiologist and a radiologist with substantial experience in PET/CT image reading. The presence of at least one suspicious lesion on full-diagnostic PET/MRI was mandatory for further evaluation.

DWI-only, PET/MRI-only, and PET/MRI with DWI images were analyzed concerning the detection and characterization of lesions. First, only the DW sequence was evaluated, with thresholds applied as mentioned below. Then, the PET/MRI with axial T2w fat-suppressed, axial LAVA, and multiplanar ceT1 were analyzed. Last, PET/MRI with DWI was evaluated.

On DWI, a malignant lesion was defined if the mean ADC (ADC_{mean}) value was lower than and 1.2×10^{-3} mm^2/s, based on reports available in the literature [17–22]. Additionally, several other thresholds were applied, ranging from 1.0×10^{-3} mm^2/s to 1.5×10^{-3} mm^2/s, in order to identify the threshold with best accuracy. So, the lesions were quantitatively defined as: 1 (higher than 1.4×10^{-3} mm^2/s); 2 (between 1.2 and 1.4×10^{-3} mm^2/s); 3 (between 1.0 and 1.2×10^{-3} mm^2/s); and 4 (lower than 1.0×10^{-3} mm^2/s).

For PET/MRI, a malignant lesion was defined based on both functional and morphological criteria. The functional criterion used for the PET compound was a maximum SUV (SUV_{max}) of at least two-fold higher than the surrounding background activity (as published before). The morphological criteria for malignancy on MRI included: (1) a mass-like lesion with irregular borders and contrast enhancement; (2) enlarged lymph nodes (LN) greater than 1.0 cm in the short axis (and 1.5 cm for angular lymph nodes), cystic, with a necrotic centre, round-shaped, in a cluster formation, with an irregular boundary of the LN capsule and/or extra capsular LN spread. If there were discordant findings between PET and MRI, the combination of the most relevant findings (morphological and functional) was taken into account (e.g., an enlarged and irregular LN was considered malignant even if there was no FDG uptake) [23].

The lesions were additionally classified both on PET/CT and MRI using a *likelihood evaluation* ranging from 1 to 4 (1, negative (meaning no suspicious lesion detected); 2, probably

benign; 3, likely (lesion likely to be malignant); and 4, very likely (lesion with very high suspicion of malignancy).

The standard of reference consisted of the histopathology (n=65) of the detected lesions, clinical evaluation (n=59), and imaging follow-up including all other imaging modalities (n=64).

ADC values were measured for each pixel with b-factors of 0 and 800 s/mm2 using the standard software on the workstation (GE Healthcare, Waukesha, WI, USA). The ADC values were evaluated within a manually drawn, oval region of interest (ROI) placed carefully within the center of the lesions, avoiding apparent cystic changes or necrosis. The b-values were also calculated using the same software after placing the ROI on the DW image (b=800 s/mm^2).

Anatomical localization, SUV_{max}, mean SUV (SUV_{mean}), ADC_{mean} ,and mean and maximum b-values (b-$value_{mean}$ and b-$value_{max}$, respectively) were also assessed.

Statistical analysis

All statistical tests were performed using SPSS Statistics Version 21 (IBM, Armonk, NY, USA). P-values<0.05 were considered statistically significant. Wilcoxon's signed-rank test was used for the comparison of the likelihood evaluation in PET/MRI and DWI. Spearman's correlation analysis was performed to evaluate the correlation between SUV_{max}, SUV_{mean}, b-$value_{max}$, b-$value_{mean}$, and ADC_{mean}. The Mann–Whitney Test was applied to analyze the difference of SUV_{max}, SUV_{mean}, b-$value_{max}$, b-$value_{mean}$, and ADC_{mean} in malignant and non-malignant lesions. McNemar's test was used to evaluate differences in the accuracy of PET/MRI and DWI compared to the standard of reference.

Results

One hundred eighty-eight (188) lesions were identified in 70 patients (53 men, 17 women; mean age 63.8 years, range 26–86 years).

The remaining 87 patients showed no FDG-positive or suspicious lesions on MRI in PET/MRI of the head and neck area, and were therefore excluded.

Of the 188 lesions, 118 were malignant (37 tumors, 74 lymph node metastases, and seven soft-tissue metastases). Of the malignant lesions, 41 lesions were confirmed by histopathology, 44 by imaging, and 33 by clinical follow-up.

Additionally, 70 benign lesions were detected (56 inflammatory/reactive lymph nodes, 10 unspecific findings, and four Whartin's tumors) and confirmed by clinical and imaging follow-up.

Of the overall 70 patients with lesions, 16 underwent imaging for primary staging and 54 for follow-up/re-staging. Mean follow-up time after PET/MRI was 196 days (range, 43 [this patient died]–394, median 180 days). Forty-one patients were alive without disease at the end of the follow-up phase, 23 were alive with disease, and six were dead as a result of disease.

The majority of the primary tumor histology (tumor histology at initial staging) was squamous-cell carcinoma (83.1 %). Overall primary tumor staging was as follows: one patient was T0 (1.6 %), 17 were T1 (26.6 %), 19 were T2 (29.7 %), nine were T3 (14.1 %), and 18 were T4 (28.1 %). The initial N-staging was N0 in 25 patients (39.1 %), N1 in eight (12.5 %), N2 in 29 (45.3 %), and N3 in two (3.1 %). The overall patient and tumor characteristics are summarized in Table 2.

PET/MRI without DWI had a higher accuracy in detecting malignant lesions than DWI alone (86.8 % vs. 60.6 %, p<0.001). PET/MRI read jointly with DWI had a slightly lower accuracy, although without statistical significance (86.8 % vs. 84.0 %, p>0.05; see Table 3). The PET/MRI likelihood evaluation was significantly different from the DWI evaluation (p=0.001; Table 4). PET/MRI was superior to DWI for all different ADC_{mean} threshold settings, mainly reflected by higher sensitivity (see Table 5).

DWI missed 48 lesions detected by PET/MRI. Thirty-one lesions were not detected by DWI due to technical reasons, such as MR artifacts (due to metal, movement) and lesion location at the edge of the field of view (FOV). The remaining 17 lesions had no restricted diffusion and were therefore missed by DWI.

Of those 48 lesions missed by DWI, 20 were malignant (nine tumors [seven recurrent and two primary], nine recurrent lymph nodes, and two metastasis). Fourteen lesions of those 20 (six tumors, six recurrent lymph nodes, and two metastasis) were missed based on technical issues (artifacts). The remaining six malignant lesions (three tumors and three recurrent lymph nodes) did not show restricted diffusion (Fig. 1).

DWI added 20 lesions to the PET/MRI findings, and of those, 11 were inflammatory/reactive lymph nodes and nine were malignant lymph nodes. However, none of these nine malignant lymph nodes changed the overall staging since other lymph nodes defining the N-stage were already detected in PET/MRI without DWI (Fig. 2).

Concerning the quantitative values of PET and DWI, there was a significant difference (p=0.001) in SUV_{max} and SUV_{mean} between malignant and non-malignant lesions (10.5 vs 6.6 and 6.4 vs 4.1, respectively). ADC_{mean} as well as b-$value_{mean}$ and b-$value_{max}$ showed no statistical significant difference between those lesions (Table 6).

PET and DWI values were significantly different between subjects referred for staging and re-staging (Table 7).

Discussion

In this study, it has been shown that PET/MRI is superior to DWI alone and that PET/MRI with DWI does not achieve a higher accuracy than PET/MRI without DWI in patients with

Table 2 Patient and tumor characteristics

No. of patients	70
Histological type, no (%)	
SCC	59 (83.1)
MEC[b], Adenocarcinoma	2 (2.8)
AdCC[b], Follicular B-cell lymphoma, odontogenic keratocyst	1 (1.4)
RMS[b], Spindle-cell-like carcinoma, melanoma, papillary carcinoma and osteosarcoma	
Primary site[a], no (%)	
Oral cavity	17 (23.9)
Mesopharynx	16 (22.5)
Epipharynx	8 (11.3)
Hypopharynx	8 (11.3)
Larynx	7 (9.9)
Maxilla	5 (7.0)
Skin	3 (4.2)
Parotid space	2 (2.8)
Thyroid, mandible, nasal cavity, CUP[b] and lymphoma involvement	1 (1.4)
Treatment, no.	
Primary staging patients (treatment after imaging)	16
- Surgery (with flap)	9 (4)
- RT	9
- CT	8
- ND	7
Re-staging patients (treatment before imaging)	54
- Surgery (with flap)	35 (16)
- RT	43
- CT	37
- ND	31
Lesions detection	188
PET/MRI and DWI	120
Only PET/MRI	48
Only DWI	20
Malignant	118
Tumor	37
Lymph node	74
Metastasis	7
Benign	70
Inflammatory/reactive	56
Unspecific	10
Whartin tumors	4

[a] 1 simultaneous SCC (Floor of the mouth and hypopharynx)

[b] *SCC* Squamous-cell carcinoma; *MEC* Mucoepidermoid carcinoma; *AdCC* Adenoid cystic carcinoma; *RMS* Rhabdomyosarcoma; *CUP* Cancer unknown primary

head and neck tumors. However, DWI is able to add different pathological lesions, although not changing the final staging. Therefore, DWI is not essential in clinical PET/MRI protocols for the staging or re-staging of head and neck cancers.

Table 3 Sensitivity, specificity, positive predictive value (PPV), negative predictive value (NPV), and accuracy of PET/MRI with DWI, PET/MRI without DWI, and DWI alone (using ADC_{mean} threshold for malignant lesions of 1,2)

	PET/MRI without DWI	PET/MRI with DWI	DWI
Sensitivity	90.4 %	99.1 %	54.8 %
Specificity	80.8 %	60.3 %	69.9 %
PPV	88.1 %	79.7 %	74.1 %
NPV	84.3 %	97.8 %	49.5 %
Accuracy	86.7 %*	84.0 %	60.6 %*

* statistically significant

General aspects

PET/MRI currently is emerging as a potential diagnostic tool that combines the functional PET information on tumor metabolism with the excellent anatomical correlation provided by different PS in MRI [13, 24, 25]. Furthermore, MRI can potentially offer additional physiological sequences that may provide information on tumor microstructure, e.g., with DWI sequences [10, 26, 27].

DWI has been promoted as a useful imaging tool to detect and characterize malignant lesions and predict tumor response in oncology [28]. In head and neck cancer single-modality MRI, DWI is often performed for tumor detection and characterization, to monitor treatment response, and for the differentiation of recurrence from post-radiation changes [11, 29, 30]. However, the quality of the DWI sequence can be severely distorted by susceptibility artifacts, particularly in the head and neck area due to dental implants, and has a relatively low specificity [29–31].

Diagnostic accuracy

In our patient population, PET/MRI had a significantly higher diagnostic accuracy and negative predictive value than DWI alone, independent of different thresholds selected for the ADC. Our study showed a DWI sensitivity varying from 44.6 to 82.2 %, depending on the ADC threshold used.

Table 4 Likelihood evaluation of PET/MRI and DWI. Numbers represent the evaluation of the lesion found in all patients (number of patients)

	PET/MRI	DWI
1 (No)	39	77
2 (Probably)	30	26
3 (Very likely)	24	28
4 (Definitely)	95	57

Table 5 Sensitivity, specificity, and accuracy of DWI with different ADC thresholds

DWI	Threshold 1.0×10^{-3} mm^2/s	Threshold 1.2×10^{-3} mm^2/s	Threshold 1.3×10^{-3} mm^2/s	Threshold 1.4×10^{-3} mm^2/s	Threshold 1.5×10^{-3} mm^2/s
Sensitivity	35.7 %	54.8 %	62.6 %	71.3 %	73.0 %
Specificity	75.3 %	69.9 %	60.3 %	50.7 %	49.3 %
Accuracy	51.1 %	60.6 %	61.7 %	63.3 %	63.8 %

However, the specificity decreases at the same time (from 65.9 % to 31.7 %). The current literature is controversial regarding ADC thresholds in oncological imaging. Razek and co-workers have shown that ADC values for residual or recurrent head and neck tumors were significantly lower than that for post-treatment changes [32]. Other publications have demonstrated that ADC was significantly higher in metastatic lymph nodes than in benign lymphadenopathy [33]. However, the ADC thresholds usually differ when analyzing HNC before treatment and after therapy [11]. Since our population includes patients referred for primary staging and for follow-up/recurrence imaging, identifying one ideal threshold value that could fit both at the same time is practically impossible. This is probably reflected in the high number of false-negative findings observed by DWI (22/142). This leads to the limited value of integrating DWI into clinical PET/MRI protocols. On the other hand, PET/MRI is able to clearly detect pathologies both during the initial staging and the follow-up using the same technique.

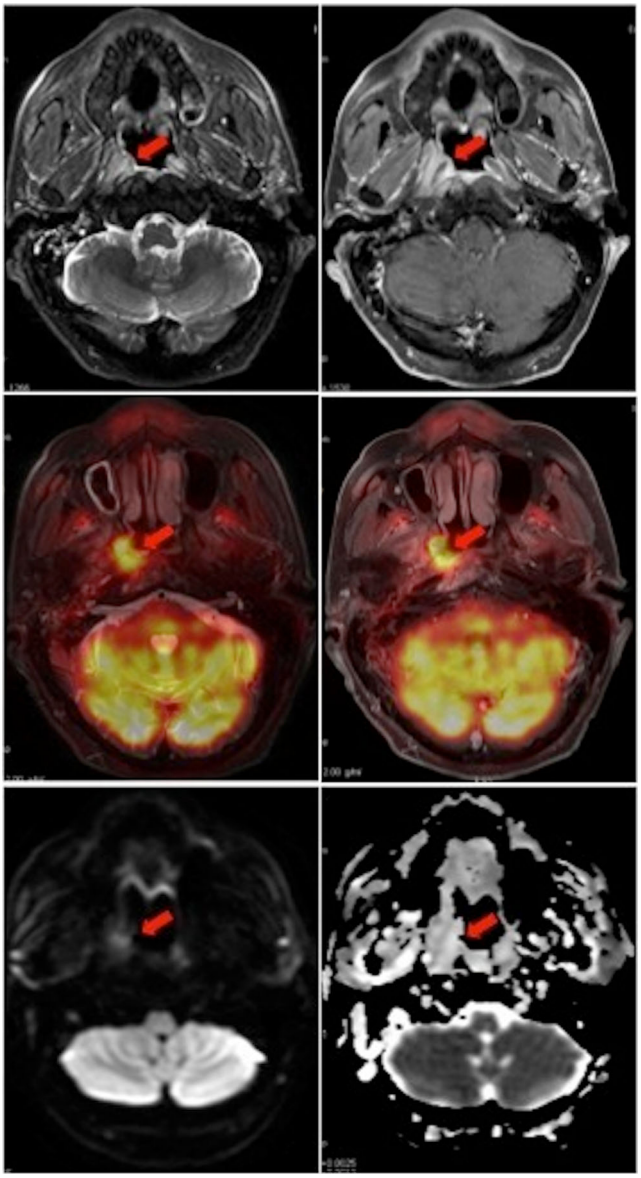

Fig. 1 Thirty-five-year-old male with recurrence of a mesopharynx carcinoma in the right rosenmuller fossa. PET/MRI accurately detected it, but DWI showed no restriction ($ADC_{mean}=1.73\times10^{-3}$ mm^2/s)

The superiority of PET/MRI as compared to DWI is also reflected by the different likelihood evaluations. It is already known that multimodality imaging provides information that is superior to morphological or functional methods alone for the detection of malignant lesions [10]. The introduction of PET/CT has demonstrated improved diagnostic performance over PET alone by reducing the number of false-positive findings in patients with initial staging and follow-up of head and neck malignancy [34, 35]. Studying a population of oro- and hypopharyngeal SCC patients, Chan and colleagues have shown that PET/CT affords higher diagnostic capability than whole-body MRI in detecting residual/recurrent tumors or associated second primary tumors [36]. However, when integrating DWI into the PET/MRI protocol in our patient population, no improvement could be found.

Malignant and non-malignant lesions

Another point regarding the ability of PET/MRI to detect and characterize malignancies was the significant difference of SUVmax between malignant and benign lesions. This finding is well-known in the PET and PET/CT literature. Ghanooni and colleagues, for example, found that SUVmax values were significantly higher in malignant than in benign, post-treatment lesions in head and neck cancer patients [37].

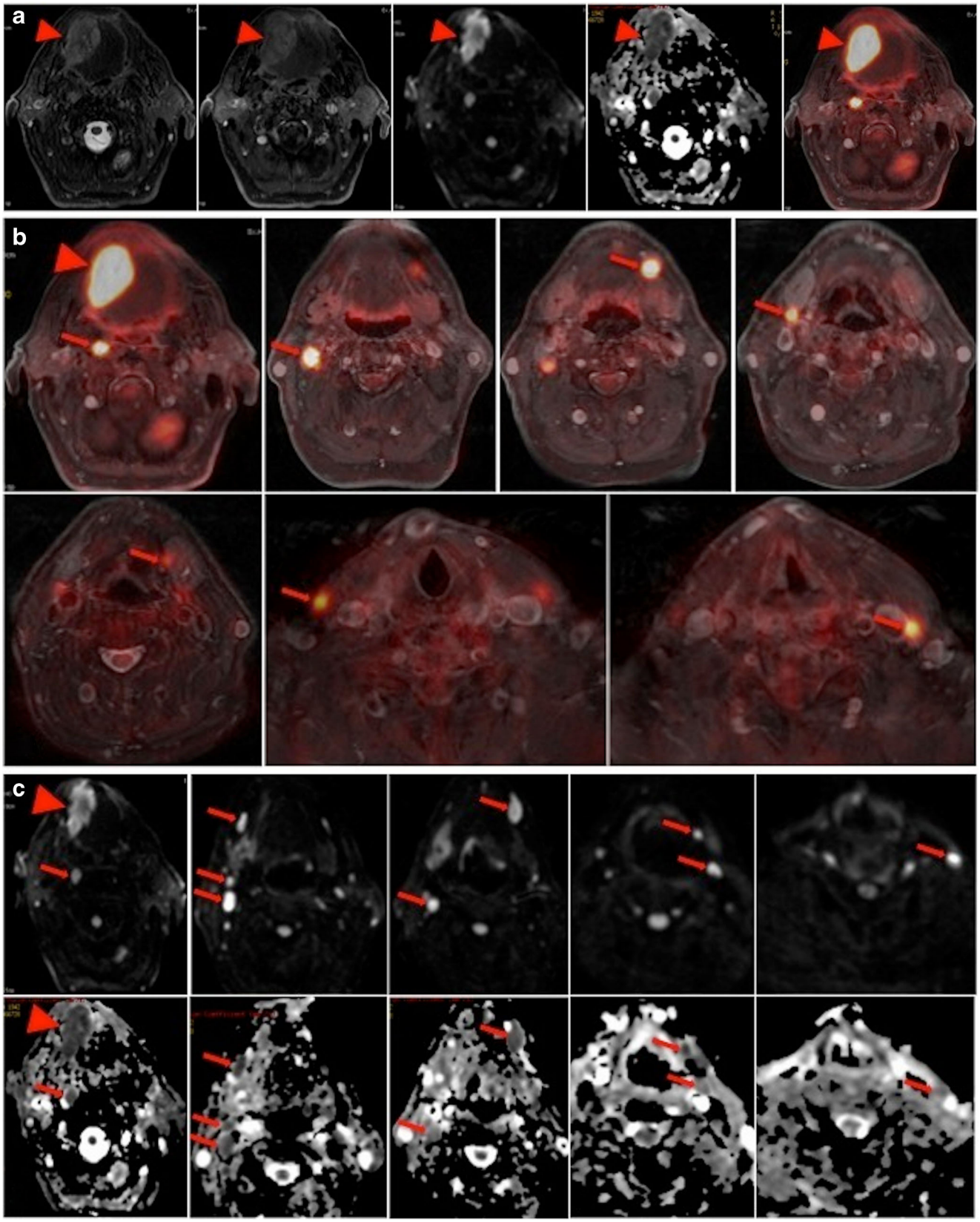

Fig. 2 **a**–**c** Sixty-nine-year-old man with squamous cell carcinoma of the base of the tongue. **a** Axial T2w, Axial ceT1w, DWI, ADC, and PET/MRI showing the primary tumor in the base of the tongue. **b** PET/MRI in different levels showing seven metastatic lymph nodes. **c** DWI (top) and ADC map (bottom) in different levels showing nine metastatic lymph nodes. In both PET/MRI and DWI, N-staging remains N2c

Table 6 Quantitative values of PET and in malignant and non-malignant lesions

	Malignant	Non-malignant	P-value
SUV max	10.5	6.6	0.001
SUV mean	6.4	4.1	0.001
ADC mean ($\times 10^{-3}$ mm^2/s)	1.19	1.15	0.299
b-value max	444.8	352	0.719
b-value mean	292.7	190.6	0.680

Conversely, the quantitative DWI parameters such as b-values and ADCs of malignant vs. benign lesions didn't show any statistical difference between malignant and non-malignant lesions. This finding is partially in contradiction to the current literature, which states that DWI is able to differentiate benign from malignant lesions in primary staging of head and neck cancers using ADC with different threshold values [6, 11], and is also able to differentiate changes related to treatment from loco-regional recurrence [32, 38]. One potential explanation for these conflicting results is that our b-values are partly lower than previously reported in the literature (800 vs. 1,000–2,000). It is known that the ADC value decreases when the b-value increases beyond 1,000 s/mm2 [30]. The decrease in the observed ADC with an increasing b-value is explained by the decay of biexponential signal intensity [30]. Thus, this requires further investigation as to whether higher b-values should be used in head and neck cancer protocols. The problem with higher b-values is that MR imaging time increases and integration into a clinically acceptable PET/MRI protocol is thus even more difficult.

PET values and DWI parameters

Our study did not show a correlation between SUV_{max} and ADC or b-values. Recent studies have demonstrated for head and neck cancers that SUVmax is inversely correlated to ADC ratio between different b-values [39] or ADC ratio between minimum and mean [40]. However, Nakajo and co-authors have shown a negative and significant correlation between SUVmax and ADC mean, studying 26 patients with HNSCC before treatment [41]. Our results are probably different due to the fact that our population is heterogenous (as it is in any clinical routine), including different histologic types of HNC and not only primary tumors.

Table 7 Quantitative values of PET and DWI in primary staging and follow-up/recurrence patients

	Primary	Follow-up	P-value
SUVmax	11.0	7.9	0.003
SUVmean	6.7	4.8	0.005
b-value max	503.5	323.9	0.016
b-value mean	338.6	178.9	0.001
ADC mean ($\times 10^{-3}$ mm^2/s)	1.06	1.27	0.035

When PET values and DWI values for different populations are compared, it has been found that they yield similar results. A malignant lesion at primary staging, for example, shows a high SUVmax and b-value, and low ADC. Thus, the information provided by DWI is superfluous, since it does not provide any information that wasn't already available from the PET/MRI.

Evaluating 30 patients with different malignancies, Borra and co-workers recently have shown the prognostic potential of b-values compared to PET uptake. The b-values represent the average signal intensity from the native DW images for each ROI, and are therefore easy to use. It was found that a high b-value was more indicative of malignant FDG uptake than the traditionally used signal loss on ADC maps [42]. However, we could not demonstrate this in our patient population with HNC. Thus, b-values might be useful in certain oncological settings, but possibly not in HNC.

Limitations

One limitation of this study was a mixed-population analysis, which included primary staging and follow-up/recurrence exams, as well as different histologic types. This might have limited the ability of the ADC threshold to differentiate benign from malignant lesions. However, it does not render the conclusion invalid, since our purpose was to evaluate the utility of DWI in a PET/MRI protocol for a routine, clinical HNC population, not specifically for primary staging or follow-up. Furthermore, different ADC thresholds were applied without significant differences concerning the overall accuracy compared to significant differences in SUV. Another limitation was the lack of pathological confirmation of all lesions, however, this is not always possible in a clinical setting. The reading process may also be considered a limitation, since two independent readers could possibly enhance the results. The DWI-only evaluation might not be highly relevant in a routine clinical setting, since DWI should be read in conjunction with a complete diagnostic MRI protocol. However, to account for similar DWI studies that are available in the current literature, it has been included.

Conclusion

The use of DWI as part of PET/MRI procedures to evaluate head and neck cancers did not provide diagnostically relevant

information in our study. Thus, the use of DWI might not be needed in clinical PET/MRI protocols for the staging or restaging of head and neck cancers.

Disclosures This research project was supported by an institutional research grant from GE Healthcare. Patrick Veit-Haibach received IIS Grants from Bayer Healthcare and Siemens Medical Solutions, and speaker fees from GE Healthcare. Gustav von Schulthess is a grant recipient of GE Healthcare funding and receives speaker fees from GE Healthcare. The other authors declare no other conflicts of interest.

References

1. Jemal A, Bray F, Center MM, Ferlay J, Ward E, Forman D. Global cancer statistics. CA Cancer J Clin. 2011;61:69–90.
2. Epidemiology and risk factors for head and neck cancer [Internet]. [cited 2014 Feb 14]. Available from: http://www.uptodate.com/contents/epidemiology-and-risk-factors-for-head-and-neck-cancer#H1.
3. Hustinx R, Lucignani G. PET/CT in head and neck cancer: an update. Eur J Nucl Med Mol Imaging. 2010;645–51.
4. Thoeny H. Diffusion-weighted MRI, in head and neck radiology: applications in oncology. Cancer Imaging. 2010;10:209–14.
5. Thoeny HC, De Keyzer F. Extracranial applications of diffusion-weighted magnetic resonance imaging. Eur Radiol. 2007;17:1385–93.
6. Srinivasan A, Mohan S, Mukherji SK. Biologic imaging of head and neck cancer: the present and the future. AJNR Am J Neuroradiol. 2012;33:586–94.
7. Friedrich KM, Matzek W, Gentzsch S, Sulzbacher I, Czerny C, Herneth AM. Diffusion-weighted magnetic resonance imaging of head and neck squamous cell carcinomas. Eur J Radiol. 2008;68:493–8.
8. Herneth AM, Guccione S, Bednarski M. Apparent diffusion coefficient: a quantitative parameter for in vivo tumor characterization. Eur J Radiol. 2003;45:208–13.
9. Higgins KA, Hoang JK, Roach MC, Chino J, Yoo DS, Turkington TG, et al. Analysis of pretreatment FDG-PET SUV parameters in head-and-neck cancer: tumor SUVmean has superior prognostic value. Int J Radiat Oncol Biol Phys. 2012;82:548–53.
10. Sadick M, Schoenberg SO, Hoermann K, Sadick H. Current oncologic concepts and emerging techniques for imaging of head and neck squamous cell cancer. GMS Curr Top Otorhinolaryngol Head Neck Surg. 2012;11:1–24.
11. Thoeny HC, De Keyzer F, King AD. Diffusion-weighted MR imaging in the head and neck. Radiology. 2012;263:19–32.
12. Buchbender C, Hartung-Knemeyer V, Beiderwellen K, Heusch P, Kühl H, Lauenstein TC, et al. Diffusion-weighted imaging as part of hybrid PET/MRI protocols for whole-body cancer staging: does it benefit lesion detection? Eur J Radiol. 2013;82:877–82.
13. Veit-Haibach P, Kuhn FP, Wiesinger F, Delso G, von Schulthess G. PET-MR imaging using a tri-modality PET/CT-MR system with a dedicated shuttle in clinical routine. MAGMA. 2013;26:25–35.
14. Kuhn FP, Crook DW, Mader CE, Appenzeller P, von Schulthess GK, Schmid DT. Discrimination and anatomical mapping of PET-positive lesions: comparison of CT attenuation-corrected PET images with coregistered MR and CT images in the abdomen. Eur J Nucl Med Mol Imaging. 2012;44–51.
15. Boellaard R, O'Doherty MJ, Weber WA, Mottaghy FM, Lonsdale MN, Stroobants SG, et al. FDG PET and PET/CT: EANM procedure guidelines for tumour PET imaging: version 1.0. Eur J Nucl Med Mol Imaging. 2010;37:181–200.
16. Kuhn FP, Wiesinger F, Wollenweber SD, Samarin A, Von Schulthess G SD. Sequential integrated PET/CT-MR system: comparison of image registration accuracy of PET/CT versus PET/MR. Melbourne, Australia: International Society for Magnetic Resonance in Medicine (ISMRM); 2012.
17. Lee M-C, Tsai H-Y, Chuang K-S, Liu C-K, Chen M-K. Prediction of nodal metastasis in head and neck cancer using a 3T MRI ADC map. Am J Neuroradiol. 2013;34:864–9.
18. Zhang Y, Chen J, Shen J, Zhong J, Ye R, Liang B. Apparent diffusion coefficient values of necrotic and solid portion of lymph nodes: differential diagnostic value in cervical lymphadenopathy. Clin Radiol. 2013;68:224–31.
19. Abdel Razek AAK, Nada N. Role of diffusion-weighted MRI in differentiation of masticator space malignancy from infection. Dentomaxillofac Radiol. 2013;42:20120183.
20. Perrone A, Guerrisi P, Izzo L, D'Angeli I, Sassi S, Mele L Lo, et al. Diffusion-weighted MRI in cervical lymph nodes: differentiation between benign and malignant lesions. Eur J Radiol. 2011;77:281–6.
21. Holzapfel K, Duetsch S, Fauser C, Eiber M, Rummeny EJ, Gaa J. Value of diffusion-weighted MR imaging in the differentiation between benign and malignant cervical lymph nodes. Eur J Radiol. 2009;72:381–7.
22. Vandecaveye V, De Keyzer F. Head and neck squamous cell carcinoma: value of diffusion-weighted MR imaging for nodal staging. Radiology. 2009;251:134–46.
23. Queiroz MA, Hüllner M, Kuhn F, Huber G, Meerwein C, Kollias S, et al. PET/MRI and PET/CT in follow-up of head and neck cancer patients. Eur J Nucl Med Mol Imaging. 2014. doi:10.1007/s00259-014-2707-9.
24. Platzek I, Beuthien-Baumann B, Schneider M, Gudziol V, Langner J, Schramm G, et al. PET/MRI in head and neck cancer: initial experience. Eur J Nucl Med Mol Imaging. 2013;40:6–11.
25. Appenzeller P, Mader C, Huellner MW, Schmidt D, Schmid D, Boss A, et al. PET/CT versus body coil PET/MRI: how low can you go? Insights Imaging. 2013;4:481–90.
26. Buchbender C, Heusner TA, Lauenstein TC, Bockisch A, Antoch G. Oncologic PET/MRI, Part 1: tumors of the brain, head and neck, chest, abdomen, and pelvis. J Nucl Med. 2012;53:928–38.
27. Chawla S, Kim S, Dougherty L, Wang S, Loevner LA, Quon H, et al. Pretreatment diffusion-weighted and dynamic contrast-enhanced MRI for prediction of local treatment response in squamous cell carcinomas of the head and neck. Am J Roentgenol. 2013;200:35–43.
28. Heijmen L, Verstappen MCHM, Ter Voert EEGW, Punt CJ, Oyen WJG, de Geus-Oei L-F, et al. Tumour response prediction by diffusion-weighted MR imaging: ready for clinical use? Crit Rev Oncol Hematol Elsevier Ireland Ltd. 2012;83:194–207.
29. Vandecaveye V, De Keyzer F, Dirix P, Lambrecht M, Nuyts S, Hermans R. Applications of diffusion-weighted magnetic resonance imaging in head and neck squamous cell carcinoma. Neuroradiology. 2010;52:773–84.
30. Hwang I, Choi S, Kim Y. Differentiation of recurrent tumor and posttreatment changes in head and neck squamous cell carcinoma: application of high b-value diffusion-weighted imaging. Am J Neuroradiol. 2013;1–7.
31. Sepahdari AR, Politi LS, Aakalu VK, Kim HJ, Abdel Razek a a K. Diffusion-weighted imaging of orbital masses: multi-institutional data support a 2-ADC threshold model to categorize lesions as benign, malignant, or indeterminate. Am J Neuroradiol. 2013;1–6.
32. Abdel Razek AAK, Kandeel AY, Soliman N, El-shenshawy HM, Kamel Y, Nada N, et al. Role of diffusion-weighted echo-planar MR imaging in differentiation of residual or recurrent head and neck tumors and posttreatment changes. Am J Neuroradiol. 2007;28:1146–52.

33. Sumi M, Sakihama N, Sumi T, Morikawa M, Uetani M, Kabasawa H, et al. Discrimination of metastatic cervical lymph nodes with diffusion-weighted MR imaging in patients with head and neck cancer. Am J Neuroradiol. 2003;24:1627–34.
34. Ishikita T, Oriuchi N, Higuchi T, Miyashita G, Arisaka Y, Paudyal B, et al. Additional value of integrated PET/CT over PET alone in the initial staging and follow up of head and neck malignancy. Ann Nucl Med. 2010;24:77–82.
35. Goerres GW, Schuknecht B, Schmid DT, Stoeckli SJ, Hany TF. Positron emission tomography/computed tomography for staging and restaging of head and neck cancer: comparison with positron emission tomography read together with contrast-enhanced computed tomography. Clin Imaging. 32:431–7.
36. Chan S-C, Wang H-M, Yen T-C, Lin C-Y, Chin S-C, Liao C-T, et al. ^{18}F-FDG PET/CT and 3.0-T whole-body MRI for the detection of distant metastases and second primary tumours in patients with untreated oropharyngeal/hypopharyngeal carcinoma: a comparative study. Eur J Nucl Med Mol Imaging. 2011;38:1607–19.
37. Ghanooni R, Delpierre I, Magremanne M, Vervaet C, Dumarey N, Remmelink M, et al. ^{18}F-FDG PET/CT and MRI in the follow-up of head and neck squamous cell carcinoma. Contrast Media Mol Imaging. 2011;6:260–6.
38. Srinivasan A, Dvorak R, Perni K, Rohrer S, Mukherji SK. Differentiation of benign and malignant pathology in the head and neck using 3T apparent diffusion coefficient values: early experience. Am J Neuroradiol. 2008;29:40–4.
39. Choi SH, Paeng JC, Sohn C-H, Pagsisihan JR, Kim Y-J, Kim KG, et al. Correlation of 18F-FDG uptake with apparent diffusion coefficient ratio measured on standard and high b value diffusion MRI in head and neck cancer. J Nucl Med. 2011;52:1056–62.
40. Ho K-C, Lin G, Wang J-J, Lai C-H, Chang C-J, Yen T-C. Correlation of apparent diffusion coefficients measured by 3T diffusion-weighted MRI and SUV from FDG PET/CT in primary cervical cancer. Eur J Nucl Med Mol Imaging. 2009;36:200–8.
41. Nakajo M, Kajiya Y. FDG PET/CT and diffusion-weighted imaging of head and neck squamous cell carcinoma. Clin Nucl Med. 2012;37:475–80.
42. Borra R, Catalano O, Catana C, McDermott S, Blake M, Sahani D, et al. Comparison of SUV and whole body diffusion imaging findings in oncological imaging with hybrid PET-MRI. Soc Nucl Med Annu Meet Abstr. 2013;54:1408.